

Constraining Gravitino Dark Matter with the Cosmic Microwave Background

Raphael Lam on

Institut für Theoretische Physik, ETH Zurich, Honggerberg, 8093 Zurich, Switzerland.

Ruth Durrer

Département de Physique Théorique, Université de Genève,
24 quai Ernest Ansermet, 1211 Genève 4, Switzerland.

(Dated: February 8, 2020)

We consider supergravity models in which the lightest supersymmetric particle (LSP) is a stable gravitino. The next-to-lightest supersymmetric particle (NLSP) freezes out with its thermal relic density and then decays after $(10^4 - 10^{10})$ sec, injecting high-energy photons into the cosmic microwave background radiation (CMB). These photons thermalize via Compton scattering, bremsstrahlung and double-Compton scattering. Contrary to previous studies which assume instantaneous energy injection, we solve the full kinetic equation for the photon number density with a source term describing the decay of the NLSP. We investigate the case of a stable NLSP and determine the constraints on gravitino and NLSP masses from observations of the CMB spectrum. In contradiction to analytical approximations with instantaneous energy injection, we find that within the interesting 100–2000 GeV mass range the modification of the CMB spectrum is very small and fully within present observational bounds, not constraining the model. However, future CMB spectrum measurements like DES can lead to very stringent bounds.

PACS numbers: 95.35.+d, 98.80.Es, 98.80.Cq

I. INTRODUCTION

Supersymmetry provides mainly two compelling candidates for cold dark matter: either the gravitino or the neutralino, depending on which one is the LSP. If we require that R-parity be conserved, the NLSP decays into the stable LSP and releases energy in standard model particles. At leading order, these late decays are two-body and the accompanying energy is mainly electromagnetic.

Part of the electromagnetic release is transferred to the cosmic microwave background radiation. The CMB then thermalizes through three relevant processes: Compton scattering ($e + e^- \rightarrow e + e^-$), double-Compton scattering ($e + e^- \rightarrow e + e^- + e + e^-$) and bremsstrahlung ($e + p \rightarrow e + p + \gamma$). The energy injection may distort the CMB, depending on the redshift at which it occurs and on the various time scales of the processes. Early NLSP decays can be fully thermalized, whereas distortions caused by injection from late decays cannot. Varying the NLSP and LSP masses, it is possible to control both the NLSP lifetime and the energy injected in the CMB.

The CMB is not only very isotropic, but it also has a very precise Planck spectrum. The FIRAS instrument aboard the COBE satellite constrained the deviation from a perfect blackbody spectrum in terms of a few numbers. Important for this work is the limit for the chemical potential [1]

$$jj \quad 9 \quad 10^5 :$$

This bound has been used to derive bounds for the energy released by NLSP decays as well as the NLSP lifetime. Observational constraints on the CMB spectrum

can be translated into bounds for the NLSP and LSP masses. Recently, several papers have employed an analytic approximation to determine these limits [2, 3, 4]. The approximation used in [2, 3, 4] is derived in Ref. [5]. This analytical result turns out to provide the most stringent limit on the gravitino dark matter model in some range for the NLSP and LSP masses. This prompted us to repeat the calculation numerically.

Surprisingly, we find that the approximate limit is significantly stronger than the bound we derive numerically. The main reason for this is the following: If the NLSP decays very early, its energy is still thermalized and no chemical potential is generated; however, if the NLSP decays late, the energy injected into the CMB does not have the time to cascade down to typical thermal energies and is not detected in a CMB experiment (it can however affect nucleosynthesis, which does lead to strong constraints as discussed in Ref. [2, 3, 4]). As we shall see, the strongest constraints come from intermediate lifetimes, but they are still in agreement with the present limit of the chemical potential.

After recalling some properties of the NLSP in the next section, we write down the full kinetic equation for the evolution of the photon one-particle distribution function in Section III. We phrase it as an evolution equation for a frequency dependent chemical potential. This allows us to determine the chemical potential for a given point in the (mass, lifetime) plane of the NLSP and to draw exclusion plots in Section IV. We summarize our conclusions in Section V.

II. NLSP PROPERTIES

We investigate a super-gravity model with a gravitino LSP and a stau NLSP. We assume that the NLSP freezes out with thermal relic density and decays after a time determined by both its mass and the LSP mass. Due to the suppression of non-photonic decay channels, the branching ratio for decays to photons is set to be equal to one.

Gravitino LSPs are produced through NLSP decays NLSP \rightarrow LSP + SM P, where SM P are standard model particles. Using the standard $N = 1$ super-gravity Lagrangian, the rates for the various decay channels of the NLSP can be calculated.

A. Slepton NLSP

The width for the decay of any sfermion f to a gravitino G for a negligible fermion mass is given by

$$(f \rightarrow f G) = \frac{1}{48 M^2} \frac{m_f^5}{m_G^2} \Gamma \left(\frac{m_G^2}{m_f^2} \right)^{\frac{1}{2}} ; \quad (1)$$

where $M = (8 G_N)^{1/2}$ is the reduced Planck mass.

Stau NLSPs decay to taus, which then decay to e^+ , e^- , and ν . As mentioned in Ref.[3], the electromagnetic energy produced in decays varies between $\frac{1}{3}E$ and $\frac{1}{2}E$. If not specified, a value of $E_M = 0.8E$ will be assumed throughout of this paper.

B. Thermal relic density

Using the thermal relic density of the right-handed slepton NLSPs determined in Ref.[6] and the thermally averaged cross section from Ref. [7], the stau relic abundance is given by

$$\frac{\Omega h^2}{\Omega_{\text{DM}}} \sim 0.2 \frac{m_{\tilde{\tau}}}{\text{TeV}}^2 : \quad (2)$$

As long as the staus do not decay, their time-dependent number density can be expressed as

$$n_{\tilde{\tau}}(t) \sim 0.26 m_{\tilde{\tau}}^3 \frac{G \text{eV}}{m_{\tilde{\tau}}} \frac{T}{\text{Kelvin}}^3 : \quad (3)$$

The fact that the final gravitino density, $\Omega_G h^2 = (m_G \Omega_{\tilde{\tau}}) \sim h^2$, is bounded by $\Omega_G h^2 \leq 0.14 \%$ together with Eq. (2) implies an upper bound for the gravitino mass as a function of the stau mass:

$$\frac{m_G}{G \text{eV}} < 0.7 \frac{10 \text{ GeV}}{m_{\tilde{\tau}}} : \quad (4)$$

III. EVOLUTION EQUATION FOR THE PHOTON NUMBER DENSITY

The decay of unstable particles into photons during the early stages of the universe can lead to distortions in the CMB. Depending on the redshift at which energy is injected, this may leave a measurable imprint of the early decays. This is the process which we now analyze in detail.

A. Energy injection by particle decays

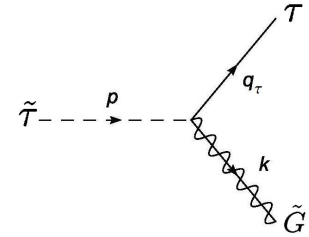


FIG. 1: Decay of a stau into a gravitino and a tau

Consider a stau of momentum p decaying into a tau of momentum q and a gravitino of momentum k , as shown in Fig. 1. The injected energy enters the Boltzmann equation as a source term given by

$$\frac{\partial}{\partial t} f_{\text{inj}}(q; t) = J(q; t); \quad (5)$$

where $J(q; t)$ denotes the number of injected particles per unit time and per volume:

$$\frac{1}{2E_q} \int \frac{d^3 p}{(2\pi)^3} \frac{1}{2E_p} \int \frac{d^3 k}{(2\pi)^3} \frac{1}{2E_k} (2\pi)^4 \delta^{(4)}(p - q - k) M^2 n(p; t); \quad (6)$$

where $n(p; t)$ is the stau distribution and M is the amplitude for decay into a gravitino and a tau. After integrating the three-dimensional delta function over the three-momentum of the gravitino k , this equation can be further simplified. Assuming that $m_{\tilde{\tau}} \gg m_{\tilde{G}}$, and setting $m_{\tilde{\tau}} = m_{\tilde{G}} = m_{\tilde{\tau}}$, we have:

$$\int j = \int j \frac{m_{\tilde{\tau}}^2 - m_{\tilde{G}}^2}{2m_{\tilde{\tau}}} = \frac{1}{2} m_{\tilde{\tau}}^2 : \quad (7)$$

Furthermore

$$q \frac{1}{m_{\tilde{G}}^2 + q^2} = q \frac{1}{2m_{\tilde{\tau}}^2 + q^2} = \frac{1 + \frac{q^2}{2m_{\tilde{\tau}}^2}}{1 + \frac{q^2}{2m_{\tilde{G}}^2}} \int j \quad (8)$$

so that

$$J(q; t) = \frac{2}{t} \frac{(\frac{2}{2+1})^{\frac{1}{2}} n_{\sim}(t)}{\int j^2} e^{t-t} \int j \frac{1}{2} m_{\sim} ; \quad (9)$$

where t_{\sim} denotes the tau lifetime,

$$t_{\sim}^{-1} = \frac{M j}{16 m_{\sim}} ; \quad (10)$$

and we have used

$$2 \frac{Z}{(2)^3} \frac{d^3 p}{2E} j^0(p; t) = 2 \frac{Z}{(2)^3} \frac{d^3 p}{2E} (p; t) \frac{d^3 p}{(2)^3} n(p; t) = n_{\sim}(t) e^{t-t} ; \quad (11)$$

The exponential factor arises due to the decay of taus and the factor 2 takes into account the anti-taus. $n_{\sim}(t)$ is the tau number density given by Eq. (3) as it would evolve without decays.

As explained above, only a fraction of the energy of the tau may be transmitted to photons. Therefore there is an additional factor $= \frac{e_M}{E}$ and the photon momentum is given by $q = q$. Substituting $\int j = xT$ where $x = h = T$ (we set $k_{\text{Boltzmann}} = 1$), we obtain for the injected photons

$$\frac{\partial n}{\partial t}_{\text{inj}} = J(q; t) = 3 \frac{2}{t} \frac{(\frac{2}{2+1})^{\frac{1}{2}}}{x^2} \frac{1}{T^3} n_{\sim}(t) e^{t-t} x \frac{1}{2T} m_{\sim} ; \quad (12)$$

The delta function in the above equation stems from the fact that we have considered a two-body decay, so the energy transmitted to the tau is fixed. However, the photons resulting from tau decays are not monochromatic due to the various decay channels of taus into photons. Therefore, the approximation of this delta function by a Gaussian, which we have to do also for numerical reasons, is well justified.

B. Photon-matter interaction

When the universe is more than a few minutes old, the coupling of CM B photons and matter is basically due to three processes: Compton scattering, double Compton scattering and bremsstrahlung. If these processes are no longer very efficient, the spectrum can be distorted. Especially, if double Compton scattering and bremsstrahlung become weak, the photon number can no longer be conserved and energy injection into the CM B leads to a chemical potential. With this in mind, we

parametrize a general distorted spectrum by a Bose-Einstein distribution with a frequency-dependent dimensionless chemical potential $(x; t)$,

$$n(x; t) = \frac{1}{\exp(x + \alpha(x; t)) - 1} ; \quad (13)$$

From observations [1] we know that $j(x; t) \approx 1$, we can thus linearize the Boltzmann equation for $n(x; t)$ in the chemical potential,

$$n(x; t) = n_0(x; t) + \alpha(x; t) \frac{\partial n_0}{\partial x} (x; t) = \frac{1}{e^x - 1} \alpha(x; t) \frac{e^x}{(e^x - 1)^2} ; \quad (14)$$

The zeroth order is the equilibrium distribution, and the first order in α describes the spectral distortion. The kinetic equations for the three relevant processes (Compton scattering, double Compton scattering and bremsstrahlung) [9], then becomes a linear equation for the evolution of the chemical potential,

$$\begin{aligned} \frac{e^x}{(e^x - 1)^2} \frac{\partial}{\partial t} (x; t) = & \frac{2}{t_e m_e} \frac{x e^{2x}}{(e^x - 1)^4} [4 \cosh x + x \sinh x]^0(x; t) x (\cosh x - 1)^{10}(x; t) \\ & + \frac{Q g(x)}{t_e} \frac{1}{x^3 (e^x - 1)} (x; t) \\ & + \frac{1}{t_e} \frac{16}{45} \frac{e_m}{m_e} \frac{T}{x^2} \frac{1}{(e^x - 1)^2} (x; t) \\ & + \frac{3}{t} \frac{2}{2+1} \frac{(\frac{2}{2+1})^{\frac{1}{2}}}{x^2} \frac{1}{T^3} n(t) e^{t-t} x \frac{1}{2T} m_{\sim} : \end{aligned} \quad (15)$$

The first term describes Compton scattering, the second bremsstrahlung, the third term double Compton scattering and the fourth is the injection term. The prime denotes a derivative w.r.t. $x = h = T$ and $t_e = (n_e p_e c)^{-1}$ is the Thomson scattering time. $Q = \frac{2}{2} \frac{2}{(m_e = T)^{1/2}} e_m n_B T^3 \approx 1.7 \cdot 10^{-10} \text{ MeV}^{-1} \text{ h}^2$ and $g(x)$ is the Gaunt factor. In order to distinguish it from the parameter introduced above, the fine structure constant is denoted by e_m . More details on the collision terms can be found in Refs. [5, 9] or [10].

We have solved Eq. (15) numerically. Some details on the numerical methods are given in Ref. [11].

C. Time evolution of the frequency-dependent chemical potential

As shown in Ref. [10], energy injected at a redshift higher than $z = 10^7$, corresponding to a time $t < t_c = 10^5$ sec is fully thermalized. Furthermore, at decoupling time $t_{\text{dec}} = 10^3$ sec, the CM B spectrum is frozen in and does not evolve anymore apart from redshifting of the photon

momenta. Therefore, the relevant temperatures range from 10^3 to 10^{-1} eV, which means that for a stau mass of $m \sim 100$ GeV, the energy injection occurs at values of $x = h = T \sim 10^6 - 10^2$. The differential equation (15) cannot be solved numerically for such high injection energies because of the exponential factors in all other terms.

Parameterizing the delta function by $(x - a)$, a numerical solution can only be found for a up to 10. This is very small compared to the real value of 10^0 . Of course at energies corresponding to $x = 10^0$ also other processes than the ones taken into account in Eq. (15) are active, but at least below $x = 100$ Eq. (15) is quite accurate. This problem can be solved by requiring that the energy injection be early enough in order for Compton scattering to be sufficiently effective to move the heated photons downward in frequency.

We have found numerically that, for sufficiently high a , the result becomes nearly independent of a . More precisely, it is possible to choose an arbitrary a as long as the stau lifetime is small compared to the freeze-out time of Compton scattering $t_{\text{freezeout}}$ and as long as a is sufficiently large so that the injection does not interfere directly with the photon-creating processes (double Compton), which are effective only at relatively low values of $x < 1$. As shown in [5], Compton scattering freezes out at $t_{\text{freezeout}} = 8 \cdot 10^8$ sec. After that time only Thomson scattering (the non-relativistic limit of Compton scattering), which does not change the photon energy remains effective until decoupling. This implies that energy injection should happen much before $t_{\text{freezeout}}$. Otherwise the injected energy remains at its high frequencies and is not detected in a CMB spectrum measurement.

The numerical result for the chemical potential at recombination (after which it remains frozen) is shown in Figs. 2 and 3 as a function of x for several values of the stau and gravitino masses and different choices of a . Clearly, the results become more and more similar with increasing a , meaning that the chemical potential should be nearly independent of the frequency at which the energy is injected, provided the injected photons are out of reach of the photon-creating processes, $a > 1$. After the injection, Compton scattering must move the injected photons downward in frequency.

Therefore, as long as Compton scattering is sufficiently effective to thermalize the photons (or equivalently, as long as the lifetime of the gravitino is not too long), the approximation of rescaling the argument in the delta function is valid for $a > 1$. However, we expect strong deviations when the gravitino lifetime is too long for Compton scattering to thermalize the photon energies. Fig. 3 confirms this expectation: energy injected at $a = 1$ for stau lifetimes $t > 10^9$ sec can no longer cascade down to low energies where it would show up as a chemical potential. Therefore, such energy injection is not detected by CMB spectrum observations.

The CMB spectrum has only been measured within the range $x \in [0.01; 10]$. For our comparison with data

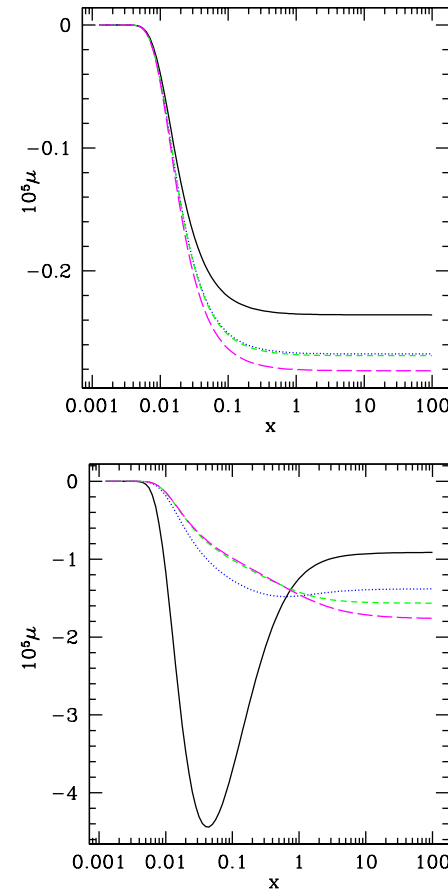


FIG. 2: The final chemical potential $(x; t_0)$ is shown as a function of the dimensionless frequency x for energy injections taking place at different dimensionless energies a . The solid (black) line corresponds to $a = 0.1$, the dotted (blue) line has $a = 1$, the dashed (green) is $a = 3$ and the long dashed (magenta) $a = 10$. Top: A stau mass of 200 GeV and gravitino mass of 20 GeV are assumed, corresponding to a lifetime of $t = 7.8 \cdot 10^5$ sec. Bottom: A stau mass of 70 GeV and gravitino mass of 25 GeV are assumed, corresponding to a lifetime of $t = 3.8 \cdot 10^8$ sec.

we therefore limit the upper frequency to $x = 10$. The shape of the curves $a = 3$ and $a = 10$ of the bottom panel of Fig. 2 close to this maximum frequency differ by about 10%. Therefore, we may only consider numerical results for a lifetime up to about $3 \cdot 10^8$ sec as accurate to about 10%. Accuracy gets rapidly worse for longer lifetimes: we see from the top panel of Fig. 3 that even constraining the frequency range to $x \in [0.01; 10]$, the results cannot be trusted if $t > 3 \cdot 10^8$ because significant energy injection occurs near the freeze-out time of Compton scattering $t_{\text{freezeout}} = 8 \cdot 10^8$ sec. We see that the low-energy injection ($a = 0.1$) is not much affected by this freeze-out because the injected photons are in the energy range where photon-creating processes are effective. However, high-energy injection, mainly at

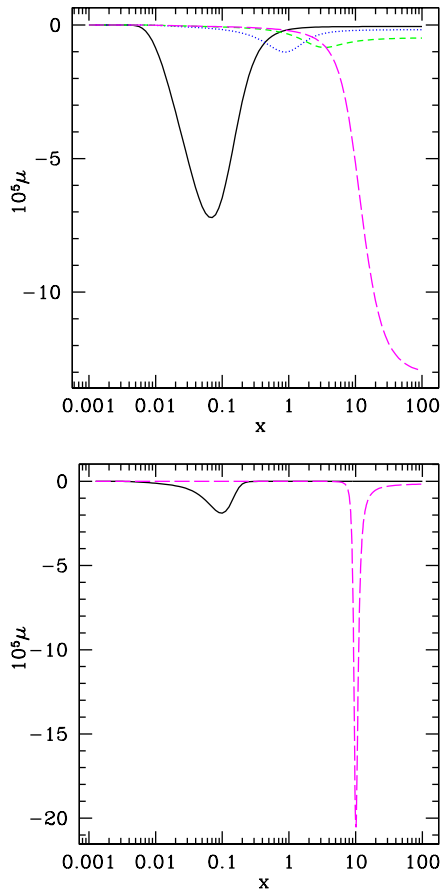


FIG. 3: Chemical potential as a function of the dimensionless frequency x for energy injections taking place at different dimensionless energies a . The colors/linestyles are like in Fig. 2. Top: A stau mass of 100 GeV and gravitino mass of 70 GeV are assumed, corresponding to a lifetime of $t = 4.3 \cdot 10^9$ sec. Bottom: Stau mass of 100 GeV and gravitino mass of 90 GeV are assumed, corresponding to a lifetime of $t = 3.7 \cdot 10^{11}$ sec.

$a = 10$, is highly affected by the freeze-out and even a Bose-Einstein spectrum with chemical potential can not be achieved. The injected photons remain nearly unmodified.

The bottom panel of Fig. 3 shows two energy injections at $a = 0.1$ and $a = 10$ for a stau lifetime $t = 3.7 \cdot 10^{11}$ sec when Compton scattering has already frozen out. While part of the low-energy injection can still be thermalized by photon-creating processes, high-energy injection at $x = 10$ remains unmodified. The injected photons are beyond reach of bremsstrahlung and Compton scattering and remain unaffected. But we know that in reality, stau decays produce electromagnetic energy not at a frequency $x = 10$, but at $x > 1000$ for lifetimes $t > 10^9$ sec. We may thus conclude that such late decays are invisible within the measured spectral range of the CMB.

Considering only the CMB constraint, we may therefore

allow stau lifetimes longer than the freeze-out time. This constraint is even weakened somewhat by the result shown in the top panel of Fig. 3: the chemical potential for an energy injection at $x = 10$ decays exponentially for decreasing x . The value at $x = 100$ is $(100; t_0) \approx 1.4 \cdot 10^4$, while at $x = 1$ it only amounts $(1; t_0) \approx 2.1 \cdot 10^6$. Energy injection at $x > 1000$ is thus completely invisible at $x < 10$ if the stau lifetime is longer than about 10^9 sec. Comparing Figs. 2 and 3, we therefore conclude that energy injection taking place after a time $t > \frac{1}{10} t_{\text{freezeout}} = 10^9$ sec has no measurable effect on the CMB spectrum.

There is an interesting interplay between a sufficiently long stau lifetime, leading to a large chemical potential (photons can no longer be generated and destroyed) and a too long stau lifetime, leading to no chemical potential at all (the injected high energy photons do not even get thermalized and never reach the low energies at which the CMB spectrum is measured). Due to this interplay there is a maximum value for the chemical potential reached in NLSP decays which is about $\mu_{\text{max}} \approx 3 \cdot 10^5$. This chemical potential is obtained for $m \approx 250$ GeV and $m_{\tilde{G}} \approx 100$ GeV, corresponding to a lifetime of $t \approx 1.5 \cdot 10^7$ sec. Contrary to the findings of the approximation which neglects the fact that too long lifetimes do not generate a chemical potential, the observational limit of $\mu \approx 9 \cdot 10^5$ cannot be reached by NLSP decays.

IV. CMB CONSTRAINTS ON THE STAU AND GRAVITINO MASSES

The FIRAS instrument aboard the COBE satellite has measured a temperature $T_0 = 2.725 \pm 0.001$ Kelvin [2], but it could only give an upper bound for the chemical potential [1, 13], $\mu < 9 \cdot 10^5$. This bound comes from measurements in the frequency range from 2 to 600 GHz, corresponding to $x = h/\lambda = T_0/2 \in [0.1; 10]$. There are still some measurements at lower frequencies, but their accuracy is worse leading to a lower bound on μ which is by at least an order of magnitude higher. To obtain good accuracy in the measured interval, we numerically compute the chemical potential for $x \in [10^{-4}; 150]$. We require that the chemical potential be never smaller than $9 \cdot 10^5$ within the experimental range $x \in [0.01; 10]$. Outside that range, μ may be larger (experiments do not rule out deviations outside the frequency range [0.5 GHz; 600 GHz]).

A point in the $(m \sim; m_{\tilde{G}})$ -plane is considered to satisfy the CMB observational bound if the magnitude of the chemical potential never trespasses the limit $9 \cdot 10^5$ within and only within the frequency range $[0.01; 10]$. Due to the criteria explained in the previous section, not every point in the $(m \sim; m_{\tilde{G}})$ -plane can be calculated, but we expect the chemical potential to be much smaller than the experimental limit for points where our calculation cannot be trusted.

An approximation of the chemical potential caused by

an instantaneous energy injection is given in [5]. However, this approximation underestimates the ability of photon-creating processes to absorb photons of a non-instantaneous energy injection. Contrary to the approximation of [5], in our numerical calculation no stau and gravitino masses can be found which generate a chemical potential lower than $9 \cdot 10^5$. We see from Eq. (10) that the lifetime increases for decreasing mass difference between the stau and the gravitino. A longer lifetime increases the magnitude of the distortions due to late decays. However, the term $(\tilde{\tau}^2 - 1)^2 = (\tilde{\tau}^2 + 1)$ in Eq. (15) which reflects the injected energy, decreases for decreasing mass difference. Therefore, there is a point where, for a constant stau mass, the magnitude of the chemical potential is maximum before decreasing for increasing gravitino mass. This maximum is $j_{\max} \approx 3 \cdot 10^5$. It is reached for $m_{\tilde{\tau}} \approx 250$ GeV and $m_{\tilde{G}} \approx 100$ GeV.

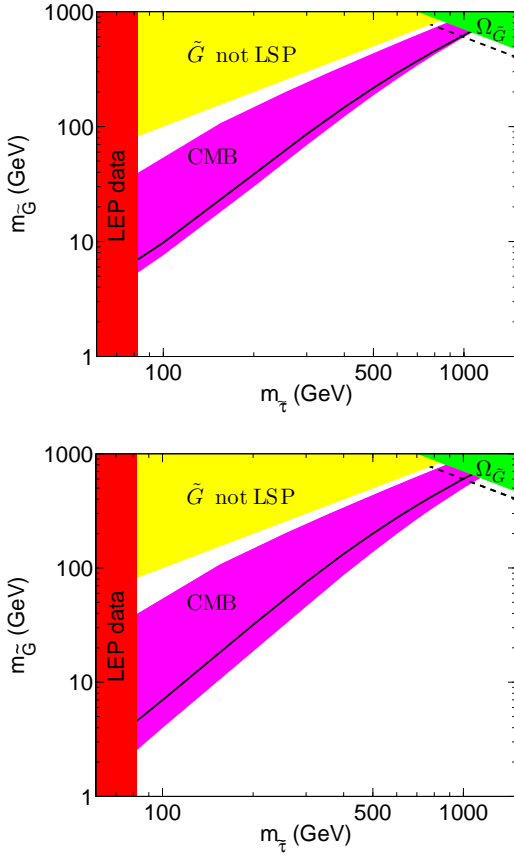


FIG. 4: Excluded and allowed regions in the $(m_{\tilde{G}}; m_{\tilde{\tau}})$ parameter space. The green region is excluded by the overclosure constraint $\Omega_{\tilde{G}} h^2 < 0.14$. The dashed line corresponds to $\Omega_{\tilde{G}} h^2 = 0.12$, the best t value for the cold dark matter density from the WMAP experiment [8]. The magenta region is forbidden for a chemical potential limit of $> 10^5$ (top) and $> 2 \cdot 10^6$ (bottom). The approximation of Ref. [5] excludes the entire region above the solid line.

Despite the fact that every point of the $(m_{\tilde{G}}; m_{\tilde{\tau}})$ parameter space is allowed by the constraint $j_{\max} < 9 \cdot 10^5$,

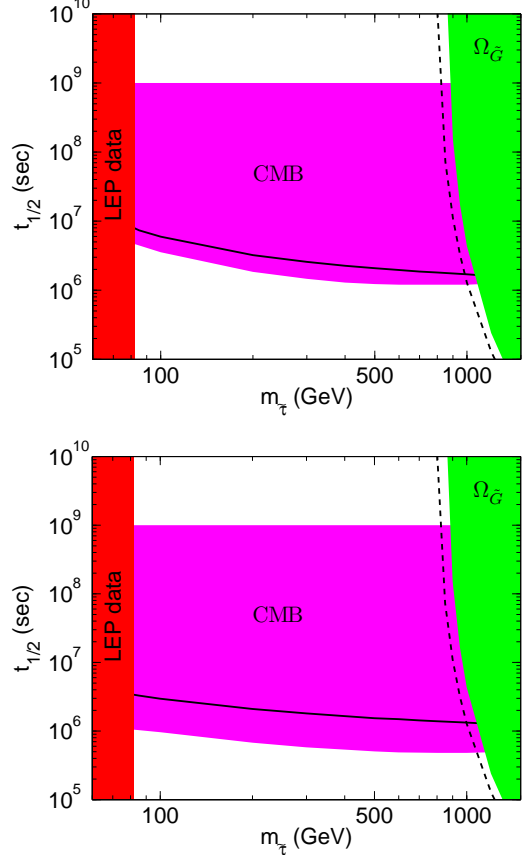


FIG. 5: Excluded and allowed regions in the $(m_{\tilde{\tau}}, \text{lifetime})$ plane for the stau. The green region is excluded by the overclosure constraint $\Omega_{\tilde{G}} h^2 < 0.14$. The dashed line corresponds to $\Omega_{\tilde{G}} h^2 = 0.12$, the best t value for the cold dark matter density from the WMAP experiment [8]. The magenta regions are forbidden for a limit on the chemical potential of $> 10^5$ (top) and smaller than $> 2 \cdot 10^6$ (bottom). The approximation of Ref. [5] excludes the entire region above the solid line.

a forbidden region can be found for $j_{\max} < 10^5$, as shown in Fig. 4 on the top panel.

The **D**isuse **M**icrowave **E**mission **S**urvey (DIME) plans to determine the CMB spectrum in the poorly studied centimeter-wavelength band, improving the limit on the chemical potential to about $j_{\max} < 2 \cdot 10^6$. If DIME does not measure distortions of the CMB, gravitinos can not significantly contribute to the missing dark matter (see Fig. 4 (bottom)).

Fig. 5 shows the allowed lifetimes for the stau as a function of its mass for two different limits on the chemical potential. For $> 10^5$, lifetimes between a few 10^6 sec and 10^9 sec are not allowed (top panel), the latter bound is caused by the freeze-out of Compton scattering, as explained above. A limit of $> 2 \cdot 10^6$ forbids lifetimes from a few 10^6 sec to 10^9 sec. Here we consider the limit for a stau mass $m_{\tilde{\tau}} = 1000$ GeV

which provides approximately the correct gravitino density, $\sigma h^2 = \sigma_{\text{CDM}} h^2 \approx 0.12$. At lower stau masses, the resulting gravitinos do not have sufficient energy and $\sigma h^2 < \sigma_{\text{CDM}} h^2$. For fixed lifetime, the chemical potential is not very sensitive to the stau mass.

V. SUMMARY

We have studied the effect on the CMB from stau NLSP decays into gravitino LSPs, assuming that the staus freeze out with their thermal relic density. We have numerically solved the kinetic equation for the photon number density with non-instantaneous energy injection. We have found that photon-creating processes are stronger than previously thought. In fact, contrary to previous results [2, 3, 4] using an approximation for the induced chemical potential [5], we have found that these

processes do not allow the chemical potential to reach the present upper bound of $\sigma h^2 < 9 \times 10^{-5}$ measured by COBE.

We conclude that the present limits on the CMB chemical potential do not constrain the gravitino mass. The present constraints on gravitino dark matter are therefore just the BBN and 'dilute photon flux' constraints discussed in Refs. [2, 3, 4]. However, should the DMES not be able to see any distortions of the black body shape of the CMB, then the gravitino LSP would be strongly constrained by the CMB spectrum.

Acknowledgments

We thank Leszek Roszkowski for bringing our attention to this problem and Jürg Fröhlich for discussions. This work is supported by the Fonds National Suisse.

[1] D. Fixsen, et al., *Astrophys. J.* **473**, 576 (1996).
 [2] J.L. Feng, A. Rajaraman, and F. Takayama, *Phys. Rev. Lett.* **91**, 011302 (2003).
 [3] J.L. Feng, A. Rajaraman, and F. Takayama, *Phys. Rev. D* **68**, 063504 (2003).
 [4] L. Roszkowski and R. Ruiz de Austri, preprint archived as hep-ph/0408227 (2004).
 [5] W. Hu, and J. Silk, *Phys. Rev. D* **48**, 485 (1993).
 [6] R.J. Scherrer, and M.S. Turner, *Phys. Rev. D* **33**, 1585 (1986).
 [7] T. Asaka, K. Hamaguchi, and K. Suzuki, *Phys. Lett. B* **490**, 136 (2000).
 [8] D.N. Spergel et al., *Astrophys. J. Suppl.* **148**, 175 (2003).
 [9] A.P. Lightman, *Astrophys. J.* **244**, 392 (1981). (There is an omission of a factor 4 in the expression for bremsstrahlung).
 [10] T. Padmanabhan, *Theoretical Astrophysics*, Vol III, Cambridge University Press, Cambridge 2002.
 [11] R. Lam, *Diploma Thesis* at ETH Zürich (2005).
 [12] J.C.M.ather et al., *Astrophys. J.* **512**, 511 (1999).
 [13] G.F. Smoot, and D. Scott in: *The Review of Particle Physics*, D.E. Groom et al., *Eur. Phys. J. C* **15**, 1 (2000); astro-ph/9711069.